Design and Operation of Four-Frequency Parametric Up-Converters*

J. A. LUKSCH†, MEMBER, IRE, E. W. MATTHEWS†, SENIOR MEMBER, IRE, AND G. A. VERWYS†, MEMBER, IRE

Summary—A theoretical analysis of a four-frequency parametric-diode up-converter is presented, retaining both sum and difference frequencies generated by mixing of pump and signal. Upper and lower sideband up-converters are compared, and it is shown that the gain limitations of the former can be overcome by combination with the latter, without appreciable loss of stability. Three different parametric amplifier configurations utilizing this four-frequency mode of operation have been designed, fabricated, and tested. These designs utilize sum-frequency up-conversion from 400 to 9400 Mc., and have exhibited noise figures below 1.5 db, gain in excess of 12 db, and bandwidths greater than 8 Mc.

I. Introduction

THE OBJECTIVE of this parametric amplifier development was to achieve low-noise operation of a UHF monopulse radar receiver. This type of radar operates by comparison of signals received on four separate antenna lobes slightly displaced from the antenna boresight axis. Sum and difference signals derived from these four through hybrids are compared after amplification to determine the location of a target with respect to the antenna axis. Accuracy of the system depends on relative stability of all components in the four amplifier channels preceding the point of comparison. It was decided to concentrate development on a sum-frequency parametric up-converter for this system, since it presumably does not involve regeneration and is therefore potentially the most stable mode of paramp operation.

II. Preliminary Development

The first up-converter constructed which yielded promising results was in the form of two crossed-waveguides, as shown in Fig. 1, with the diode mounted in an aperture between them. This configuration incorporates sufficient tuning flexibility that it should be possible to match the pump, sum, and signal frequencies and short circuit the difference frequency simultaneously, as assumed in the usual theoretical analysis for this mode of operation. A signal around 400 Mc was introduced coaxially through a double-stub tuner, and a pump frequency of 9 kMc was used, so the output sum-filter was tuned to 9400 Mc. After adjusting the short circuit in the pump waveguide to yield a good match for the pump input, the sum-frequency output

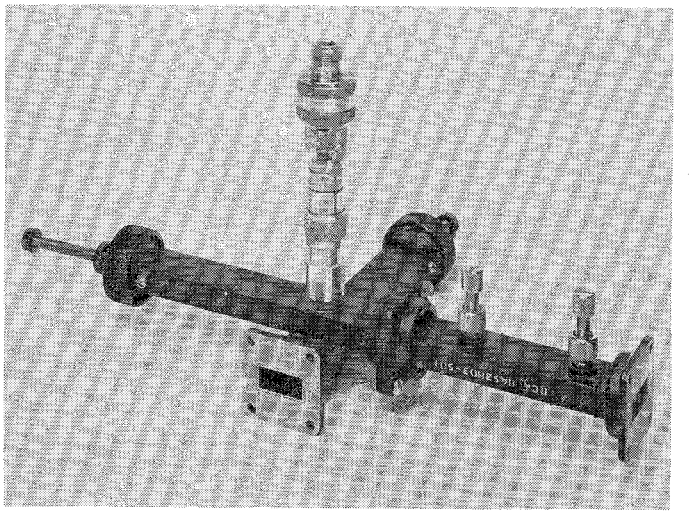

Fig. 1—Crossed waveguide amplifier.

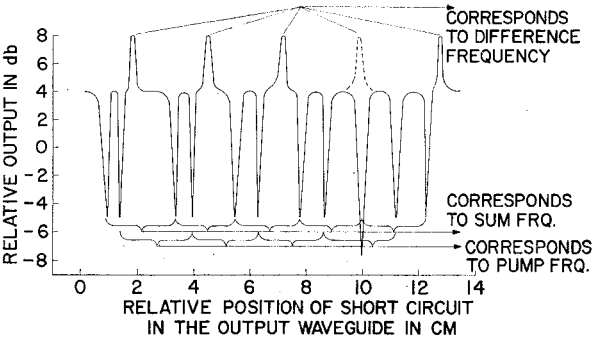

Fig. 2—Tuning of sum-frequency mode of operation of parametric amplifier.

was found to vary, as shown in Fig. 2, with movement of the short circuit in the output waveguide. It was observed that the peaks of maximum output were separated by one-half wavelength at the *difference* frequency (8600 Mc), and the maximum gain was found to be *more* than the 13-db maximum predicted by the Manley-Rowe energy relations. This indicated that internal regeneration was taking place, and that a more complete theoretical investigation was needed to understand the phenomenon.

III. Theoretical Investigation

Some insight into the operation of a four-frequency parametric amplifier may be gained by consideration

* Received by the PGMTT, June 15, 1960; revised manuscript received, September 21, 1960.
† Missile and Surface Radar Div., Defense Electronic Products, Radio Corp. of America, Moorestown, N. J.

of the Manley-Rowe[1] power relations as they apply to a lossless diode. If transfer of power is allowed only at signal, pump, sum, and difference frequencies, these relations reduce to

$$\frac{W_s}{f_s}+\frac{W_+}{f_+}-\frac{W_-}{f_-}=0 \quad \text{(a)}$$
$$\frac{W_p}{f_p}+\frac{W_+}{f_+}+\frac{W_-}{f_-}=0 \quad \text{(b)}, \tag{1}$$

where positive values of W represent power absorbed by the diode. The first equation may be rearranged to obtain the up-converter power gain G_p^+, as[2]

$$G_p^+ = -\frac{W_+}{W_s}=\frac{f_+}{f_s}-\left(\frac{W_-}{W_s}\right)\left(\frac{f_+}{f_-}\right). \tag{2}$$

This indicates that the gain at the sum frequency is increased if power is removed at the difference frequency, and if the regeneration is controlled so that W_s remains positive (*i.e.*, the signal input conductance remains positive). Eq. 1(b) indicates that the pump power will have to increase to supply the additional output at both sum and difference frequencies.

The equivalent circuit shown in Fig. 3 may be considered for this four-frequency mode of operation. The equations for the 3-port diode network of Fig. 3, considering it to be lossless, can be expressed as

$$\begin{aligned} I_s &= jB_{11}V_s + jB_{12}V_+ + jB_{13}V_- \\ I_+ &= jB_{21}V_s + jB_{22}V_+ + jB_{23}V_- \\ I_- &= jB_{31}V_s + jB_{32}V_+ + jB_{33}V_-. \end{aligned} \tag{3}$$

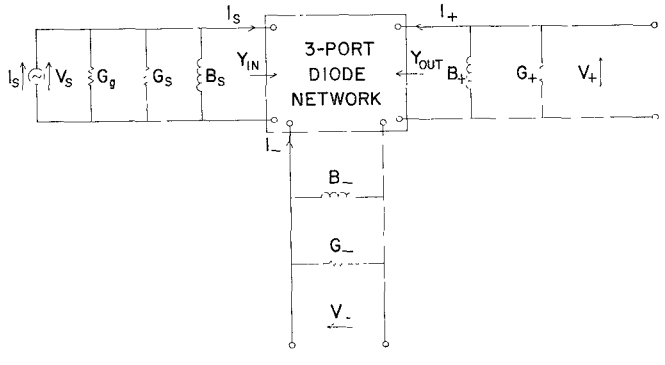

Fig. 3—Four-frequency paramp equivalent circuit.

With the terminal loads indicated in Fig. 3 connected to the diode network, the circuit equations can be solved for the signal input admittance Y_{in} as

$$Y_{in}(s)=\frac{I_s}{V_s}=jB_{11} + \frac{B_{13}B_{31}Y_2+B_{12}B_{21}Y_3-j(B_{12}B_{23}B_{31}+B_{13}B_{32}B_{21})}{Y_2Y_3+B_{32}B_{23}}, \tag{4}$$

where $Y_2=G_++jB_++jB_{22}$ and $Y_3=G_-+jB_-+jB_{33}$. Now if B_+ and B_- are adjusted for tuning the amplifier so that $B_+=-B_{22}$ and $B_-=-B_{33}$, then $Y_2=G_+$ and $Y_3=G_-$ and (4) becomes

$$Y_{in}(s)=jB_{11} + \frac{B_{13}B_{31}G_++B_{12}B_{21}G_--j(B_{12}B_{23}B_{31}+B_{13}B_{32}B_{21})}{G_+G_- + B_{32}B_{23}}. \tag{5}$$

The available power gain of the amplifier for sum-frequency up-conversion, defined as the ratio of power output at f_+ to the power absorbed at f_s, is given by

$$G_p^+ = \left|\frac{V_+}{V_s}\right|^2 \frac{G_+}{G_{in}} \tag{6}$$

where

$$G_{in} = \text{R.P.}(Y_{in}) = \frac{B_{13}B_{31}G_+ + B_{12}B_{21}G_-}{G_+G_- + B_{32}B_{23}} \tag{7}$$

and B_s is adjusted to tune out the susceptive part of Y_{in}.

$\frac{V_+}{V_s}$ can be obtained from the network equations (3) as

$$\frac{V_+}{V_s}=\frac{-B_{23}B_{31}-jB_{21}G_-}{G_+G_- + B_{23}B_{32}}, \tag{8}$$

so that (6) becomes

$$G_p^+ = \frac{G_+(B_{23}^2B_{31}^2 + B_{21}^2G_-^2)}{(G_+G_- + B_{23}B_{32})(B_{13}B_{31}G_+ + B_{12}B_{21}G_-)}. \tag{9}$$

This choice of gain definition is perhaps most representative of the amplifier capabilities, since it represents the power gain which can be obtained if the generator is matched to the amplifier input.

The diode network coefficients in (3) can be obtained according to the procedure outlined by Leenov, *et al.*,[3] assuming a lossless diode being driven by a large pump voltage $v_p(t)$ and a small signal voltage $v_s(t)$ so that the voltage across the diode is

$$v(t) = V_{dc} + v_p(t) + v_s(t) \tag{10}$$

where V_{dc} is the bias voltage and $v_s(t)$ includes small amplitude modulation products.

[1] J. M. Manley and H. E. Rowe, "Some general properties of nonlinear elements—Part I. General energy relations," PROC. IRE, vol. 44, pp. 904–913; July, 1956.

[2] E. M. T. Jones and J. S. Honda, "A low noise up-converter parametric amplifier," 1959 IRE WESCON CONVENTION RECORD, pt. 1, pp. 99–107, with proper corrections. Parts of the theoretical development which follows also closely parallels that of D. K. Adams, "An analysis of four-frequency nonlinear reactance circuits," IRE TRANS. ON MICROWAVE THEORY AND TECHNIQUE, vol. 8, pp. 274–283; May, 1960.

[3] D. N. Leenov, A. Uhlir, Jr., and A. E. Bakanowski, Bell Tel. Labs. Interim Rept. on Task 8, Signal Corps Contract No. DA-36-034-SC 65589; 1954 to present.

The charge on the capacitor is some function of this voltage $v(t)$. If the pump voltage is much larger than the signal voltage, this charge function may accurately be expanded in a Taylor's series about $v_p(t)$, and $v_s(t)$ may be considered a small variation about this expansion point, or

$$Q(t) = f(v) = f(v_p) + f'(v_p)v_s(t) + 1/2f''(v_p)v_s^2(t) + \cdots. \quad (11)$$

Neglecting terms in $v_s^2(t)$ and higher, the coefficient $f'(v_p)$ represents the variable capacitance $C(t)$ seen by $v_s(t)$ and produced by $v_p(t)$. If $v_p(t)$ is expressed as a Fourier series of fundamental frequency b,

$$v_p(t) = \sum_{n=-\infty}^{\infty} v_n e^{j2\pi nbt}, \quad (12)$$

$f'(v_x)$ may be similarly expanded as

$$f'(v_p) = C(t) = \sum_{n=-\infty}^{\infty} C_n e^{j2\pi nbt}, \quad (13)$$

where $C_{-n} = C_n$ if $C(t)$ is assumed to be an even function.

The small signal voltage $v_s(t)$ includes all frequencies which result from the conversion process, except the pump and its harmonics, so that

$$v_s(t) = \sum_{k=\pm 1} \sum_{m=-\infty}^{\infty} v_{km} e^{j2\pi(mb+ks)t}. \quad (14)$$

The small-signal charge variations are given by

$$Q_s(t) = C(t)v_s(t) = \sum_{k=\pm 1} \sum_{m=-\infty}^{\infty} \sum_{n=-\infty}^{\infty} C_n v_{km} e^{j2\pi[(m+n)b+ks]t} \quad (15)$$

and the corresponding current is obtained from

$$i_s(t) = \frac{dQ_s(t)}{dt}. \quad (16)$$

The current components of interest are those at the signal, sum, and difference frequencies, which may be found from (15) and (16):

$$\begin{aligned} I_s &= jw_sC_0V_s + jw_sC_1V_+ + jw_sC_1V_-^* \\ I_+ &= jw_+C_1V_s + jw_+C_0V_+ + jw_+C_2V_-^* \\ I_-^* &= -jw_-C_1V_s - jw_+C_2V_+ - jw_-C_0V_-^*. \end{aligned} \quad (17)$$

Comparing (17) with (3) yields the following values for the diode network parameters:

$$\begin{aligned} B_{11} &= w_sC_0 & B_{12} &= w_sC_1 & B_{13} &= w_sC_1 \\ B_{21} &= w_+C_1 & B_{22} &= w_+C_0 & B_{23} &= w_+C_2 \\ B_{31} &= -w_-C_1 & B_{32} &= -w_-C_2 & B_{33} &= -w_-C_0. \end{aligned} \quad (18)$$

Substituting these values into the gain and input conductance expressions, (7) and (9), yields

$$G_p^+ = \left(\frac{w_+}{w_s}\right) \frac{1}{1 - \left(\frac{w_-}{w_+}\right)\left(\frac{G_-}{G_+}\right)\left(\frac{G_+^2 + w_+^2C_2^2}{G_-^2 + w_-^2C_2^2}\right)} \quad (19)$$

$$G_{\text{in}} = (w_sC_1^2) \frac{w_+G_- - w_-G_+}{G_+G_- - w_+w_-C_2^2}. \quad (20)$$

The corresponding gain expression for operation in the difference-frequency mode (power output at w_-, power dissipated at w_+) is

$$G_p^- = \left(\frac{w_-}{w_s}\right) \frac{1}{\left(\frac{w_+}{w_-}\right)\left(\frac{G_+}{G_-}\right)\left(\frac{G_-^2 + w_-^2C_2^2}{G_+^2 + w_+^2C_2^2}\right) - 1}. \quad (21)$$

The negative term in the denominator of each of the gain expressions indicates the presence of regeneration in both the sum and difference frequency types of operation. The input conductance expression (20), with difference terms in both numerator and denominator, suggests the possibility of obtaining stable operation with positive input conductance at the signal terminals while operating with appreciable regeneration and consequent high gain for either sum or difference frequency output. If the signal input conductance is negative, the above gain expressions are meaningless, since no net signal power is absorbed by the amplifier. In this case, the transducer gain may be used; this is defined as the ratio of the up-converter power output to the power available from the signal source. For the sum-frequency type of operation, this transducer gain is given by

$$\begin{aligned} G_t^+ &= \frac{|V_+|^2G_+}{I_g^2/4G_g} = \frac{4G_gG_+}{I_g^2}\left|\frac{V_+}{V_s}\right|^2\left|\frac{I_s}{G_{\text{in}}}\right|^2 \\ &= \frac{4G_gG_+}{(G_g + G_s + G_{\text{in}})^2}\left|\frac{V_+}{V_s}\right|^2 = \frac{4G_g|G_{\text{in}}G_p^+|}{(G_g + G_s + G_{\text{in}})^2} \end{aligned} \quad (22)$$

where G_g and G_s are as shown in Fig. 3, and G_p^+ is the value obtained from (19), which is actually negative.

The diode losses can be included in the analysis if the self-admittance terms in (3) are assumed to contain an added conduction component ($jB_{11} \rightarrow G_{11} + jB_{11}$). The input conductance then becomes

$$G_{\text{in}} = G_{11} + (w_sC_1^2) \frac{w_+(G_- + G_{33}) - w_-(G_+ + G_{22})}{(G_+ + G_{22})(G_- + G_{33}) - w_+w_-C_2^2}. \quad (23)$$

The available power gain for sum-frequency output becomes

$$G_p^+ = \left(\frac{w_+}{w_s}\right)\left(\frac{G_+}{G_+ + G_{22}}\right)\left[1 + \left(\frac{G_{11}}{G_+ + G_{22}}\right)\frac{[(G_+ + G_{22})(G_- + G_{33}) - w_+w_-C_2^2]^2}{w_sw_+C_1^2[w_-C_2^2 + (G_- + G_{33})^2]} - \left(\frac{G_- + G_{33}}{G_+ + G_{22}}\right)\left(\frac{w_-}{w_+}\right)\frac{w_+^2C_2^2 + (G_+ + G_{22})^2}{w_-^2C_2^2 + (G_- + G_{33})^2}\right]^{-1}. \quad (24)$$

If G_{11} can be neglected (since the diode Q will be the greatest at the signal frequency), (24) becomes

$$G_p^+ = \left(\frac{w_+}{w_s}\right)\left(\frac{G_+}{G_+ + G_{22}}\right)\frac{1}{1 - \left(\frac{G_- + G_{33}}{G_+ + G_{22}}\right)\left(\frac{w_-}{w_+}\right)\frac{w_+^2C_2^2 + (G_+ + G_{22})^2}{w_-^2C_2^2 + (G_- + G_{33})^2}}. \tag{25}$$

These equations including moderate diode loss are of the same form as the original equations neglecting loss, the primary difference being an increase in each of the circuit conductance components by the amount of the diode conductance at the respective frequencies.

The variation of gain and input conductance of a four-frequency upper-sideband up-converter are plotted in Figs. 4, 5, and 6 as functions of the difference-frequency loading (G_-), for typical values of G_+, C_1, and C_2 and a lossless diode. The fundamental pump-frequency component of capacitance variation C_1 does not appear in the gain expression (19) and does not affect the sign of the input conductance (20). The second-harmonic capacitance variation C_2, together with the conductances G_+ and G_-, control both gain and input conductance. The equations are plotted for pump and signal frequencies of 9000 and 400 Mc, respectively, corresponding to the frequencies used in the experimental amplifiers described later. The three figures represent progressively increasing values of G_+, with the same value of C_1 and C_2. Figs. 4 and 6 show positive regions of input conductance for large and small values of G_-, separated by a region of negative input conductance. The transitions between these regions coincide with the points of infinite gain and represent the points where either the numerator or denominator of of the input conductance expression (20) changes sign. These points can be made to coincide by the proper choice of G_+ and C_2, as shown approximately in Fig. 5; in this case, no negative input conductance will be observed for any value of G_- (except the one singular point), and the amplifier will be unconditionally stable. Otherwise, there will be two regions of stable operation separated by one of unstable operation, as in Figs. 4 and 6. In either case, the possibility definitely exists of a choice of operating conditions which will yield high

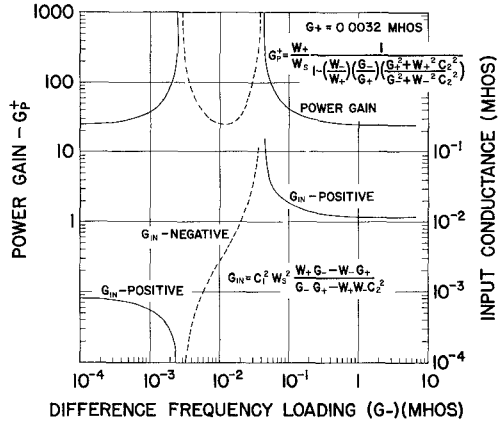

Fig. 4—Characteristics of sum-frequency up-converter.

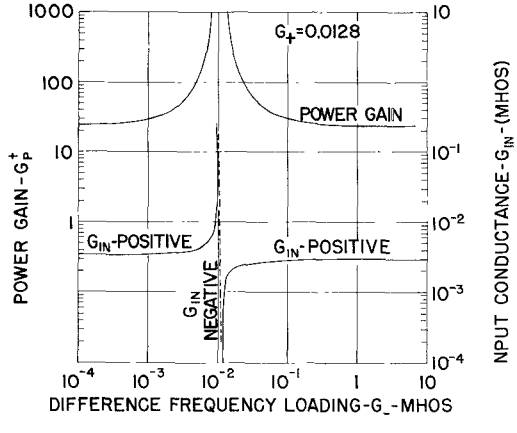

Fig. 5—Characteristics of sum-frequency up-converter.

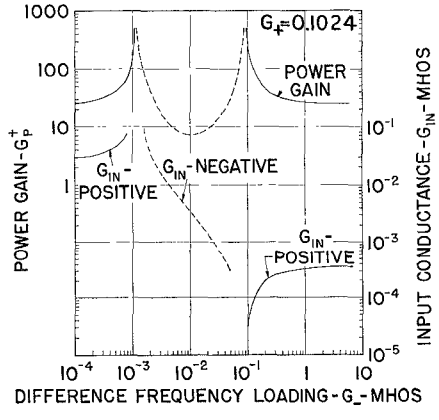

Fig. 6—($G_+ = 0.1024$) Characteristics of sum-frequency up-converter.

gain, with regeneration, but without negative input signal conductance, and consequently stable operation.

The form of the gain equation (21) for difference-frequency output is the same as that for sum-frequency operation (19), and the same input conductance expression (20) applies, so that the two types of operation would exhibit similar characteristics, with slightly higher gain for the sum frequency because of the greater up-conversion ratio. It is interesting to note that while absorption of power at the difference frequency produces increased gain for the sum-frequency up-converter, absorption of power at the sum frequency tends to stabilize the operation of the difference-frequency up-converter. Furthermore, since the diode resistance dissipates power at all frequencies, this may produce both effects naturally.

The effect of pump power variation on the gain of the sum-frequency mode is shown in Fig. 7. The primary effect of pump power is to change the diode coefficients C_0, C_1 and C_2. A change of C_0 will affect amplifier tuning at all frequencies, while a change of C_1 will affect match conditions at all frequencies. The variation of C_2 will alter the regeneration condition, and thus will be most important in determining over-all performance.

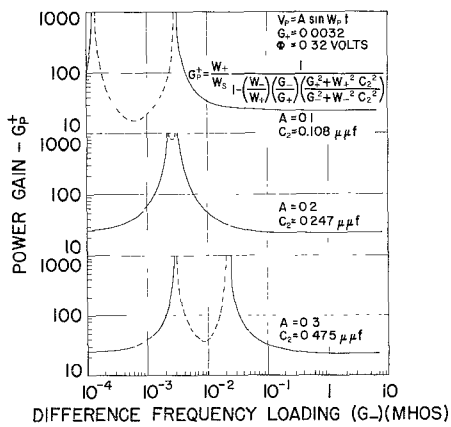

Fig. 7—Pump-power gain variation of up-converter.

Fig. 7 shows the variation of gain as a function of G_- for three different values of C_2, representing three different pump-power levels. The characteristics of these curves are the same as those in Figs. 4–6, showing two gain peaks, one of which remains fixed with varying C_2, while the other moves, and can coincide with the first for a critical value of C_2. The values of the diode coefficients can be obtained numerically as a function of pump-power level, if the diode characteristic is known. The values shown in Fig. 7 assume the usual relation for a linearly-graded junction diode:

$$C = \frac{C'}{\sqrt[3]{1 - \frac{V}{\phi}}} \tag{26}$$

with $C' = 1$ pfd, $V_{Bias} = 0$, and $\phi = 0.32$ volt.

The importance of including C_2, the second harmonic variation of the variable capacitance, in the analysis of this four-frequency operation is apparent from the major role it plays in determining input conductance, gain, and consequently stability. In fact, control of the amplifier characteristics by direct injection of a second harmonic component of pump voltage has been suggested. It may be necessary to consider even higher pump harmonics in order to obtain ultimate agreement with experiment.

Experimental results have shown that the dissipation of power at the fourth frequency in the up-converter operation does not degrade the noise performance to any measurable extent. Jones and Honda[2] have derived noise figure equations for this four-frequency mode, neglecting the C_2 terms, with similar conclusions.

The noise figure equation for sum-frequency up-conversion is most easily derived if the network equations (3) are altered to include the terminating impedances, so that

$$jB_{11} \rightarrow G_g + G_s + G_{ds} + jB_s + jB_{11}, \text{ etc.,} \tag{27}$$

where G_{ds} is the diode loss at the signal frequency. If the susceptances are tuned out, the real coefficients remaining on the principal diagonal may be identified as

$$\begin{aligned} G_1 &= G_g + G_s + G_{ds} \\ G_2 &= G_+ + G_{d+} \\ G_3 &= G_- + G_{d-}. \end{aligned} \tag{28}$$

The matrix currents now represent externally applied currents.

The noise figure may be defined as

$$F = \frac{\text{Total noise power delivered to the load } (G_+)}{\text{Noise power delivered to the load from } G_g}.$$

Using (28) and the previous notation, this can be derived as

$$F = 1 + \frac{G_{ds}}{G_g} + \frac{G_3}{G_g}\frac{(C_2^2G_1^2 + w_s^2C_1^4)}{C_1^2(G_3^2 + w_-^2C_2^2)} + \frac{G_2}{G_g}\frac{(G_1G_3 - w_sw_-C_1^2)^2}{w_+^2C_1^2(G_-^2 + w_-^2C_2^2)}. \tag{29}$$

Neglecting diode losses and loss due to signal input loading G_s, this may be evaluated for the high-gain condition[4] as

$$F = 1 + \frac{w_+G_+(w_s^2C_1^4 + G_g^2C_2^2)}{w_-G_gC_1^2(w_+^2C_2^2 + G_+^2)} + \frac{G_+\left(\frac{G_gG_+}{w_+} - w_sC_1^2\right)^2}{G_g\ C_1^2(w_+^2C_2^2 + G_+^2)}. \tag{30}$$

[4] Since the poles of the gain expression (19) coincide with the poles and zeros of the input conductance (20), the high-gain condition may be arbitrarily identified with the zero-input conductance condition. This condition may be used to relate G_- to G_+ and eliminate the former from (29).

Examination of (30) reveals that the noise figure decreases for decreasing G_+ and increasing w_+, and that there is an optimum relationship among the parameters which will eliminate the last term in (30).

If the following set of typical values is substituted into (30), the potential noise figure neglecting losses is under 0.2 db: $C_1=0.25$ pfd.,/$C_2=0.05$ pfd./$f_s=400$ Mc, $f_p=9$ kMc, $G_+=10^{-4}$ mhos, and $G_s=10^{-2}$ mhos.

The operating characteristics of an actual four-frequency up-converter depend on the individual control of each of the four frequencies involved. The extent to which such independent control is possible depends on the configuration chosen. In the following section, experimental results will be presented for three different physical configurations, and a comparison of their performances will be made.

IV. Experimental Results

A. Crossed-Waveguide Type

The crossed-waveguide UHF up-converter on which four-frequency operation was first observed was incorporated into a complete receiver system according to the block diagram of Fig. 8. The X-band local oscillator signal was derived by combining a UHF local oscillator signal with the pump frequency; this produces an IF output independent of pump frequency, and is the first step towards stable up-converter operation. The necessary filters and isolators were incorporated as shown to prevent undesired interaction between various parts of the system. The balanced mixer and 60-Mc IF preamplifier had a combined noise figure of about 9 db, and with the amplifier tuned to a center frequency of around 400 Mc, the system had an over-all gain and noise figure variation with frequency as shown in Fig. 9.[5] This represents a tuning condition for a maximum up-converter gain of about 22 db, with a 3-db bandwidth of 8 Mc, and a system noise figure at midband of less than 1 db. The varactor diodes used were Microwave Associates MA-460F or Sylvania D4110D, for which a pump power of under 10 mw was required. The variation of gain and noise figure with pump power for this amplifier are shown in Fig. 10; both variations are fairly linear with pump power near the specified operating point, and a change of ± 5 per cent in pump power causes a change in gain of ± 3.5 db.

Equivalent performance of this amplifier could be obtained over a 50-Mc band with only two tuning adjustments required—position of the short circuit in the output waveguide (tuning the difference frequency) and adjustment of the UHF input tuner. By completely retuning filters and mixers (whose bandwidths were about 100 Mc), it was possible to achieve nearly equivalent performance at L-band (1000 Mc), with only a slight degradation of noise figure to about 1.5 db.

B. Balanced Type

A balanced diode mount utilizing a pair of varactor diodes with an X-band hybrid as shown in Fig. 11 was constructed for operation as a four-frequency up-converter. The advantage expected from this type of operation is isolation between pump and sideband signals produced by the hybrid because of the relative phases involved. This isolation, however, is strongly dependent upon balancing of the two diodes and their associated input circuits. Additional isolation of the sum-frequency output from the pump was provided by means of a movable cutoff-type high-pass filter consisting of a section of small-size waveguide designed to slide within the standard waveguide, as shown in Fig. 11. This adjustability provides for reflective tuning of the difference frequency to control the internal regeneration. The individual diode mounts were designed for a good match to the pump and sum frequencies, while a double-tuned lumped constant circuit was used to match the diodes to the coaxial input.

Measured characteristics of this amplifier, incorporated into the same system described for the crossed-waveguide unit, are shown in Fig. 12. The maximum gain obtained was only about 12 db, and the minimum noise figure about 3 db, nearly half of which was contributed by the mixer IF stages following. This reduced performance in comparison with the crossed-waveguide type was partially caused by the fact that only one reversed pair of MA-460D diodes (60 kMc cutoff) was available for these tests. Furthermore, the balance conditions of the two diodes in actual operation could not be checked easily and would certainly affect the regenerative operation considerably.

The stability of this configuration against changes in pump power are shown in Fig. 13. The operation appears extremely stable—a pump power of 10 mw produced optimum noise figure, while an increase to 40 mw did not produce oscillation. The noise figure was under 4.0 db, for pump powers between 5 and 25 mw, a remarkable range.

C. Circulator Type

The third up-converter configuration investigated utilized an X-band circulator to separate the pump and sum-frequency output signals as shown in Fig. 14. A single varactor diode is used in an X-band mount, which is matched for both pump and sum frequencies; this is coupled to one arm of the circulator through a movable cutoff-type high-pass filter which reflects the difference frequency to provide the internal regeneration. Input signal tuning was by means of a coaxial double stub tuner. The performance obtained with an

[5] Gain of the up-converter was measured by the standard technique of inserting a known attenuation in the X-band output line and measuring the change in combined amplifier-mixer noise figure. The gain thus measured corresponds to the transducer gain as defined in (22), which is by its definition equal to or less than the available power gain, depending upon conditions of input match.

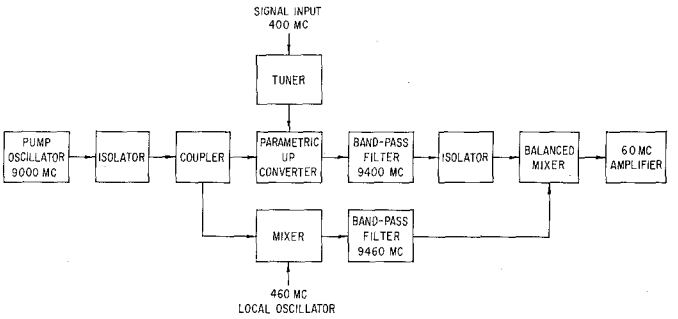

Fig. 8—Receiver system block diagram.

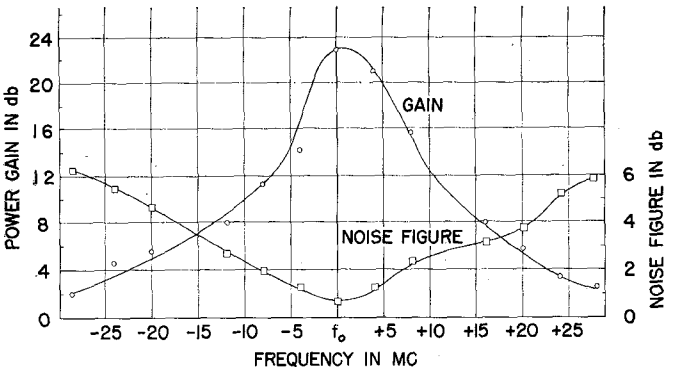

Fig. 9—Gain and noise figure of crossed-waveguide up-converter.

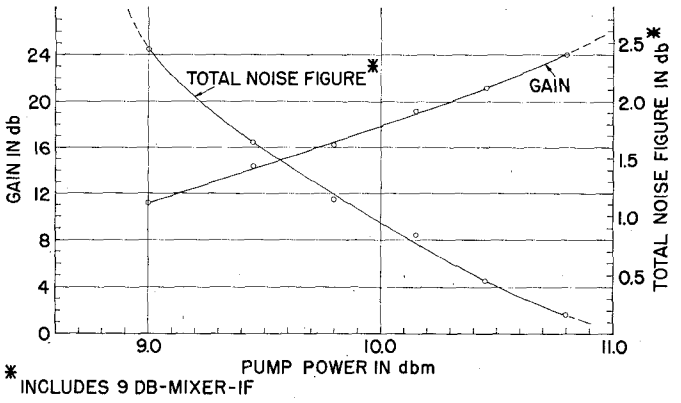

Fig. 10—Variation of gain and noise figure of parametric amplifier vs pump power (crossed-guide).

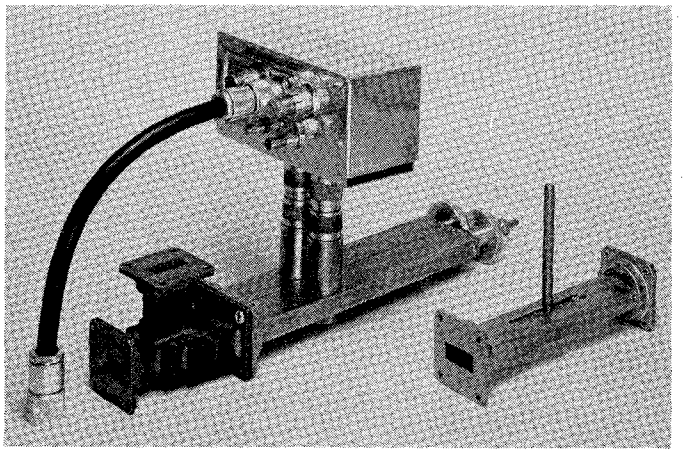

Fig. 11—Balanced amplifier.

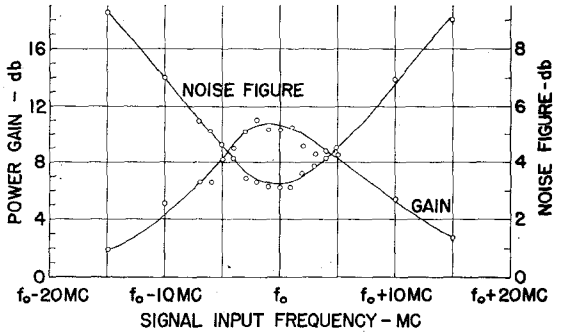

Fig. 12—Band-pass characteristics, balanced amplifier.

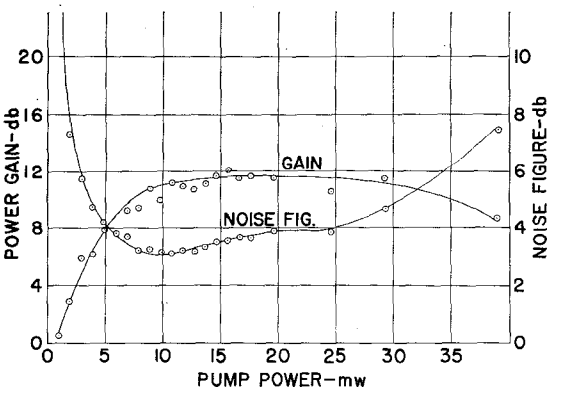

Fig. 13—Gain and noise figure vs pump-power level, balanced amplifier.

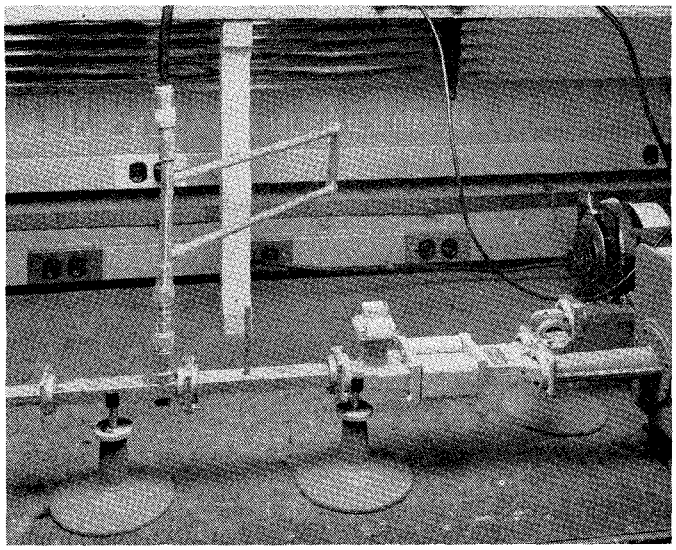

Fig. 14—Circulator-type amplifier.

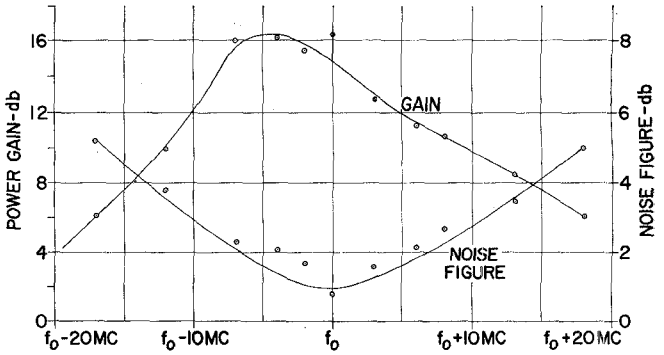

Fig. 15—Band-pass characteristics, circulator-type amplifier.

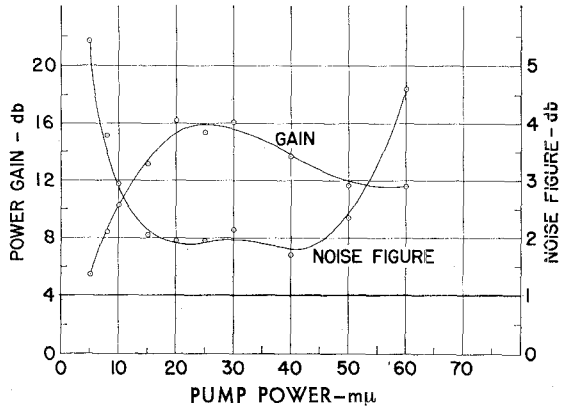

Fig. 16—Gain and noise figure vs pump-power level, circulator-type amplifier.

MA-460F varactor is shown in Fig. 15. A maximum up-converter gain of 20 db was achieved, with a 3-db bandwidth of 12 Mc and a receiver noise figure under 1 db at midband. Tuning of this unit was extremely easy and involved readjustment of signal input tuner and movable high-pass filter.

Equivalent performance could be achieved over a range of at least 50 Mc. The stability with pump-power variation is shown in Fig. 16. Nominal pump power required was about 25 mw, higher than the other configurations because of circulator loss and mismatch of the high-pass sliding filter. This power could fluctuate ± 25 per cent ($\sim$1 db) with very little change in amplifier gain or noise figure. Further increase in pump power did not produce oscillation.

A summary of the operating characteristics of the three up-converters is shown in Table I. The dynamic range for linear operation of all three types appears to be from the noise level to the point where the output approaches a level 25 to 30 db below the pumping level. This represents a range of about 75 db for a system bandwidth of the order of 5 Mc.

The over-all stability of these up-converter systems was investigated by building two of the crossed-waveguide types, operating them from common pump and signal sources, and comparing their outputs at IF. Operation of the two was adjusted in phase and amplitude to produce a null in the comparison circuit. This null was maintained to within $\pm 3°$ in phase and ± 0.5 db in amplitude over a period of several hours without adjustment, using a temperature-stabilized reflex klystron with a well-regulated power supply for the pump source.

TABLE I

Characteristics of Four-Frequency UHF Parametric Up-Converters

Type	Signal Frequency Mc	Gain db	Noise* Figure db	Bandwidth Mc	Pump Power mw
Crossed Waveguide	400	22	1.0	8	10
	1000	20	1.5	—	20
Balanced	400	12	3	9	10
Circulator	400	16	1	12	25

* Mid-band noise figure including contribution of 9 db mixer—IF combination.

D. Correlation with Theory

Correlation between the above experimental results and the theoretical results derived in the previous section is exceedingly difficult to make. First of all, it is necessary to know the equivalent circuit parameters for the configuration tested, such as G_+, G_-, G_g, and G_s. Next, the diode parameters C_1 and C_2 must be determined under actual operating conditions, as they depend on pump power level, bias, diode characteristics, and relative loading at each harmonic of the pump frequency. Diode losses would complicate the analysis tremendously. An analysis similar to that of Knechtli

and Weglein[6] would assist in the evaluation, but would be considerably more complicated for the four-frequency type of operation.

Consequently, the authors feel that the theoretical results are most useful in predicting the type of operation which might be expected from a four-frequency parametric amplifier (and which might explain some inconsistencies in supposedly three-frequency operation). Meanwhile, the experimental results represent typical values obtained in the laboratory. Other configurations, particularly those which permit more independent control of tuning and loading of each of the four frequencies, and which perhaps allow some measure of independent control of the diode coefficients C_1 and C_2, may produce superior results and may be easier to correlate with theory.

Further experiments with the crossed-guide and circulator type paramps mentioned above have shown that for best noise performance the amplifier adjustments seem to produce a regenerative gain at the signal input port of about 8 db, when the up-converter gain is about 20 db. The difference of 12 db is within 2 db of the theoretical gain due to up-conversion alone. This appears to indicate that best noise performance is obtained in the potentially-unstable region of negative input conductance, in Figs. 4 and 6. Correlation with theory would have to be made in terms of transducer gain, as in (22). Because of the negative input conductance, it has been found very necessary to operate these amplifiers with an isolator on the signal input port to provide stability against input mismatch over the entire frequency band of the amplifier, particularly for use with a radar having many wavelengths of transmission line between the actual antenna and the parametric amplifier.

[6] R. C. Knechtli and R. D. Weglein, "Low-noise parametric amplifier," PROC. IRE, vol. 48, pp. 1218–1226; July, 1960.

V. Acknowledgment

The authors wish to thank V. Stachejko for his excellent design and experimental work on the crossed-waveguide unit and R. M. Scudder for his guidance and suggestions. Portions of this paper have been incorporated into a master's thesis submitted to the University of Pennsylvania by two of the authors.

Ferrites with Planar Anisotropy at Microwave Frequencies*

ISIDORE BADY†, SENIOR MEMBER, IRE

Summary—**Materials with an easy plane of magnetization (planar anisotropy) have recently been discovered. The large anisotropy field that tends to keep the magnetization in the easy plane reduces the field required to cause ferromagnetic resonance, which makes the material promising for microwave applications. Equations are derived for the susceptibility, taking into account losses and a finite medium. Propagation in a longitudinal and transverse static field is considered. The location of a slab in a rectangular waveguide for minimum loss in the forward direction, and the use of the material as a phase shifter, are discussed. Experimental microwave data on some materials are given, and also data on an isolator and phase shifter incorporating these materials.**

* Received by the PGMTT, June 10, 1960; revised manuscript received, August 1, 1960.

† United States Army Signal Res. and Dev. Lab., Fort Monmouth, N. J.

I. Introduction

FOR most ceramic magnetic materials used in the microwave frequency range, the magnetic anistropy field is sufficiently small so that it can be neglected in deriving equations for engineering applications. However, there are two groups of materials that have very large anisotropy fields that cannot be neglected. Both of these groups have a hexagonal crystal structure; the first has an easy direction of magnetization along the C axis, and the second has an easy plane of magnetization perpendicular to the C axis (planar anisotropy). The first group includes the ceramic permanent magnetic material, barium ferrite, marketed under various trade names such as Ferroxdure, Magnadur, Indox, Ceramagnets, etc. The latter group is called Ferrox-